



Title	The RhoA regulators Myo9b and GEF-H1 are targets of cyclic nucleotide-dependent kinases in platelets
Authors(s)	Comer, Shane, Nagy, Zoltan, Bolado, Alfonso, Smolenski, Albert P., et al.
Publication date	2020-11
Publication information	Comer, Shane, Zoltan Nagy, Alfonso Bolado, Albert P. Smolenski, and et al. "The RhoA Regulators Myo9b and GEF-H1 Are Targets of Cyclic Nucleotide-Dependent Kinases in Platelets." Wiley, November 2020. https://doi.org/10.1111/jth.15028 .
Publisher	Wiley
Item record/more information	http://hdl.handle.net/10197/12616
Publisher's statement	This is the peer reviewed version of the following article: Comer, S, Nagy, Z, Bolado, A, et al. The RhoA regulators Myo9b and GEF H1 are targets of cyclic nucleotide dependent kinases in platelets. J Thromb Haemost. 2020; 00: 1– 11, which has been published in final form at https://doi.org/10.1111/jth.15028 . This article may be used for non-commercial purposes in accordance with Wiley Terms and Conditions for Self-Archiving.
Publisher's version (DOI)	10.1111/jth.15028

Downloaded 2026-05-01 23:42:56

The UCD community has made this article openly available. Please share how this access benefits you. Your story matters! (@ucd_oa)



© Some rights reserved. For more information

The RhoA regulators Myo9b and GEF-H1 are targets of cyclic nucleotide-dependent kinases in platelets

Shane Comer^{*,†}, Zoltan Nagy^{*,‡}, Alfonso Bolado[§], Alexander von Kriegsheim[§], Stepan Gambaryan[¶], Ulrich Walter^{**}, Oliver Pagel^{††}, René P. Zahedi^{††,‡‡}, Kerstin Jurk^{**}, and Albert Smolenski^{*,†}

Affiliations

^{*}UCD School of Medicine and Conway Institute, University College Dublin, Belfield, Dublin 4, Ireland;

[†]Irish Centre for Vascular Biology, Royal College of Surgeons in Ireland, 123 St Stephen's Green, Dublin 2, Ireland;

[‡]Institute of Experimental Biomedicine, University Hospital and Rudolf Virchow Center Würzburg, University of Würzburg, Josef-Schneider-Straße 2, 97080 Würzburg, Germany;

[§]Cancer Research UK Edinburgh Centre, University of Edinburgh, Crewe Road South, Edinburgh EH4 2XR, UK;

[¶]Sechenov Institute for Evolutionary Physiology and Biochemistry, Russian Academy of Sciences, 44 Thorez Prospect, St. Petersburg, 194223 Russia;

^{**}Center for Thrombosis and Hemostasis, University Medical Center Mainz, Langenbeckstrasse 1, 55131 Mainz, Germany;

^{††}Leibniz-Institut für Analytische Wissenschaften-ISAS-e.V., Otto-Hahn-Str. 6b, 44227 Dortmund, Germany;

^{‡‡}Segal Cancer Proteomics Centre, Lady Davis Institute, Jewish General Hospital, McGill University, 3755 Côte Ste-Catherine Road, Montreal, Quebec H3T 1E2, Canada

Running title: RhoA regulation by Myo9b and GEF-H1 in platelets

Corresponding author

Albert Smolenski
UCD Conway Institute
UCD School of Medicine
University College Dublin,
Belfield, Dublin 4
Ireland
e-mail: albert.smolenski@ucd.ie
phone: (353) 1-716-6746.

Essentials

- The endothelium inhibits platelets via cyclic nucleotide dependent pathways.
- cAMP and cGMP dependent protein kinases (PKA, PKG) inhibit the GTPase RhoA in platelets.
- RhoA regulation does not involve phosphorylation of RhoA.
- Phosphorylation of the RhoA regulators Myo9b and GEF-H1 mediates RhoA inhibition by PKA and PKG.

Abstract

Background

Circulating platelets are maintained in an inactive state by the endothelial lining of the vasculature. Endothelium-derived prostacyclin and nitric oxide stimulate cAMP- and cGMP-dependent kinases, PKA and PKG, to inhibit platelets. PKA and PKG effects include the inhibition of the GTPase RhoA which has been suggested to involve the direct phosphorylation of RhoA on serine 188.

Objectives

We wanted to confirm RhoA S188 phosphorylation by cyclic nucleotide-dependent kinases and to identify possible alternative mechanisms of RhoA regulation in platelets.

Methods

Phosphoproteomics data of human platelets was used to identify candidate PKA and PKG substrates. Phosphorylation of individual proteins was studied by Western blotting and Phos-tag gel electrophoresis in human platelets and transfected HEK293T cells. Pull-down assays were performed to analyse protein interaction and function.

Results

Our data indicate that RhoA is not phosphorylated by PKA in platelets. Instead, we provide evidence that cyclic nucleotide effects are mediated through the phosphorylation of the RhoA-specific GTPase-activating protein Myo9b and the guanine nucleotide exchange factor GEF-H1. We identify Myo9b S1354 and GEF-H1 S886 as PKA and PKG phosphorylation sites. Myo9b S1354 phosphorylation enhances its GAP function leading to reduced RhoA-GTP levels. GEF-H1 S886 phosphorylation stimulates binding of 14-3-3 β and has been shown to inhibit GEF function by facilitating binding of GEF-H1 to microtubules. Microtubule disruption increases RhoA-GTP levels confirming the importance of GEF-H1 in platelets.

Conclusion

Phosphorylation of RhoA regulatory proteins Myo9b and GEF-H1, but not RhoA itself, is involved in cyclic nucleotide mediated control of RhoA in human platelets.

Keywords

phosphorylation, Cyclic AMP-Dependent Protein Kinases, Cyclic GMP-Dependent Protein Kinases, GTPase-Activating Proteins, Guanine Nucleotide Exchange Factors, 14-3-3 Proteins

Introduction

Platelets play crucial roles in haemostasis, thrombosis and inflammation. In healthy, intact vasculature, the endothelial lining of blood vessels constantly releases prostacyclin (PGI₂) and nitric oxide (NO). These factors contribute to the regulation of platelet function and haemostasis, by maintaining platelets in their inactive state (1-3). PGI₂ binds to a Gs-coupled receptor thus stimulating cAMP synthesis by adenylate cyclase. NO diffuses through the cellular membrane and activates soluble guanylate cyclase (sGC) to produce cGMP. cAMP and cGMP activate cyclic nucleotide-dependent kinases, PKA and PKG, resulting in the phosphorylation of downstream substrate proteins. This ultimately causes the inhibition of platelet adhesion, aggregation and granule release. The list of potential PKA/PKG substrates in human platelets continues to expand (4), however, verification of substrates and understanding of functional consequences of phosphorylation events are still limited (1).

The GTPase RhoA is a known target for regulation by cyclic nucleotide pathways. RhoA functions as a molecular switch by cycling between its active (RhoA-GTP) and inactive (RhoA-GDP) states which is controlled by GTPase activating proteins (GAPs) and guanine nucleotide exchange factors (GEFs). Various platelet agonists such as thrombin and thromboxane A₂ have been shown to increase RhoA-GTP levels in human platelets (5-7) while cyclic nucleotide signalling inhibits RhoA activation (8). Megakaryocyte specific mouse knockout models indicate that RhoA is critical to platelet biology with RhoA depleted platelets showing reduced myosin light chain (MLC) phosphorylation, reduced integrin activation and impaired shape change in response to agonists (6, 9). The direct phosphorylation of RhoA on S188 by PKA/PKG has been proposed as a mechanism of RhoA inhibition (10). PKA mediated RhoA S188 phosphorylation was stipulated to inhibit membrane localisation of RhoA leading to MLC phosphatase activation, dephosphorylation of MLC and reduced stress fibre formation (11). Similar findings were obtained for PKG effects on RhoA in platelets (12, 13). Interestingly, NO-induced RhoA inhibition was described to be independent of RhoA S188 phosphorylation (13). Recent phospho-proteome analyses of PKA/PKG signaling in human platelets provided no evidence for RhoA phosphorylation ((3, 4, 14) and SG, UW, OP, RPZ, KJ, unpublished).

Alternative ways of regulating small GTPases might involve specific regulatory GAP or GEF proteins. We have previously shown that GAPs and GEFs of Rac1 (15), G_q and G_i (16), and Rap1B (17) are substrates for PKA/PKG phosphorylation in platelets. Little data on RhoA specific GAPs or GEFs in platelets is available so far (7, 18, 19). In this study we show that human platelets express Myo9b (unconventional myosin IXb), a myosin motor protein containing a RhoA specific GAP domain (20), and GEF-H1 (ARHGEF2), a microtubule regulated RhoA specific GEF (21). We provide evidence that PKA and PKG phosphorylate Myo9b and GEF-H1 in platelets leading to altered GAP and GEF functions that could contribute to RhoA inhibition.

Methods

cDNA constructs and site-directed mutagenesis

Human eGFP-GEF-H1 construct has been described previously (22). FLAG-tagged human Myo9b was obtained from GenScript Biotech (OHu04432, Piscataway NJ, USA). eGFP-

tagged human Myo9b was obtained by sub-cloning into eGFP-C1 using the Gibson assembly protocol[©] according to manufacturer's protocol (E5510, New England Biolabs). eGFP-tagged rat Myo9b homologue was kindly provided by Martin Bähler (23). Glutathione-S-transferase-(GST)-14-3-3 β was prepared as described previously (17). GST-Rhotekin-Rho-binding-domain (GST-RBD) was kindly provided by Harry Mellor (University of Bristol, UK). Point mutations were introduced into constructs by PCR using primers carrying the desired changes and PfuUltra High-fidelity DNA Polymerase (Agilent). WT plasmids were digested with DpnI restriction enzyme (Thermo Scientific) and mutants were grown in One Shot TOP10 chemically competent *E. coli* (Thermo Fisher Scientific). Mutagenesis was confirmed by DNA sequencing (Eurofins Genomics).

Antibodies

Mouse anti-RhoA (sc-418, Santa Cruz Biotechnology), rabbit anti-phospho-RhoA (S188) (ab41435, Abcam, and orb335688, Biorbyt), rabbit anti-Rap1 (sc-65, Santa Cruz Biotechnology), rabbit anti-Rap1GAP2 (IG-1024, custom made by ImmunoGlobe), rabbit anti-phospho-Rap1GAP2 (S7) (UDU-1-50-1, custom made by Epitomics/Abcam), rabbit anti-Myo9b (12432-1-AP, Proteintech), rabbit anti-GEF-H1 (55B6, Cell Signaling Technology), rabbit anti-phospho-GEF-H1 (S886) (E1L6D, Cell Signaling Technology), rabbit anti-GFP (ab290, Abcam) were used as primary antibodies. For blots detected using enhanced chemiluminescence (ECL) method, horseradish peroxidase-coupled donkey anti-mouse, anti-rabbit IgG (715-035-150, 711-035-152, Jackson ImmunoResearch Europe Ltd.) or donkey anti-goat IgG (sc2020, Santa Cruz Biotechnology) secondary antibodies were used. For blots detected using LI-COR Odyssey scanning system, IRDye 680LT goat anti-mouse IgG (926-68020, LI-COR) and IRDye 800CW goat anti-rabbit IgG (926-3221, LI-COR) secondary antibodies were used.

Cell culture and Platelet preparation

HEK293T were cultured using Dulbecco's modified Eagle's medium including 10% foetal bovine serum and 1% penicillin/streptomycin (41965-039, 10270-106, 15070-063, Thermo Fischer Scientific) at 37 °C and 5% CO₂ in air. Transient transfection was performed using PolyJet reagent (SL100688-05, SignaGen Laboratories) and cells were harvested on the following day. Primary platelets were obtained from healthy donors who had given their informed consent under the Declaration of Helsinki and with ethical approval from University College Dublin (LS-08-13-Smolenski, LS-19-68-Smolenski). 40 ml of venous blood was drawn into a 50 ml tube containing 10 ml of CCD-EGTA buffer (100 mM tri-sodium citrate, 7 mM citric acid, 140 mM glucose, 15 mM EGTA). For Phos-tag analysis, 10 ml CCD-EGTA buffer was substituted with 8.4 ml of ACD buffer (85 mM tri-sodium citrate, 65 mM citric acid, 100 mM glucose). Blood samples were aliquoted into 15 ml tubes (8 ml per tube) and centrifuged at 200 RCF at room temperature (RT; approx. 18°C) for 15 minutes without the brake. The upper platelet-rich plasma (PRP) layer was separated from other blood components and re-centrifuged at 600 RCF at RT for 10 minutes. Pelleted platelets were resuspended in prewarmed (37°C) platelet resuspension buffer (pH 7.4; 145 mM NaCl, 1mM MgCl₂, 5 mM KCl, 10 mM glucose, 10 mM HEPES). Platelets were incubated at 37°C and ambient air for 35-50 minutes before treatment and lysis.

Cell treatment and lysis

HEK293T cells were incubated with 10 μ M forskolin in DMEM for 10 min at 37°C and washed twice with chilled phosphate-buffered saline or, in case of Phos-tag analyses, with tris-buffered saline. Platelets were incubated in resuspension buffer with 0.5 μ M or 50 nM PGE1 (P5515-1MG, Sigma-Aldrich) for 30 seconds or 15 minutes, 10 μ M forskolin (F6886-10MG; Sigma-Aldrich) for 10 minutes, 10 μ M SNP (31444-50G, Sigma-Aldrich) for 10 minutes, 0.1 U/ml thrombin (10602400001, Sigma-Aldrich) for 1 minute, 1 μ M U46619 (16450, Cayman Chemical) for 1 minute or 10 μ M nocodazole (SML 1665, Sigma-Aldrich) for 1 minute, all at 37°C.

Cells were lysed either in standard lysis buffer (150 mM NaCl, 50 mM Tris-HCl (pH 7.5), 5 mM MgCl₂, 1% Triton X-100) or, for RhoA-GTP assays, in Rap lysis buffer (200 mM NaCl, 50 mM Tris-HCl (pH 7.4), 2.5 mM MgCl₂, 10% (v/v) glycerol, 1% (v/v) Nonidet P-40) supplemented with Complete Mini EDTA Free protease inhibitor cocktail tablets (11836170001, Roche) and PHOSSTOP phosphatase inhibitor tablets (4906837001, Sigma-Aldrich). For dephosphorylation experiments, lysate samples were treated with λ protein phosphatase as described in the manufacturer's protocol (P0753S, New England Biolabs). Lysed cell samples were centrifuged at 13,200 RPM at 4°C for 10 mins to remove cellular debris.

Pull-down assays and immunoprecipitation

Pull down assays of RhoA-GTP levels and 14-3-3 binding were performed using glutathione-S-transferase (GST)-RBD and GST-14-3-3 β fusion proteins. Fusion proteins were expressed in BL21 (DE3) E.coli (C2527H, New England Biolabs) and purified from bacterial lysates using GSH-4B resin (17075601, GE Healthcare). 10 μ l of GST-RBD or GST-14-3-3 β saturated GSH resin were added to cell lysates and incubated at 4°C for 1 hour (GST-RBD) or overnight (GST-14-3-3 β). Resin was then washed using lysis buffer, PBS with 1% Triton X-100 and PBS. Immunoprecipitation of eGFP-tagged proteins was performed by adding 4 μ l of GFP-Trap_A beads (gta-20, Chromotek) to cell lysates and incubating for 1 hour at 4°C. Beads were then washed with lysis buffer, PBS with 1% Triton X-100 and PBS. For Phos-tag PAGE PBS was replaced by TBS in all wash buffers. All precipitated samples were boiled at 95°C with 3XSDS sample buffer for SDS-PAGE or Phos-tag PAGE preparation.

Phos-tag gel electrophoresis

Phos-tag gel electrophoresis and blotting were performed as previously outlined (24). Specific gel running times and transfer times were optimised for individual proteins: RhoA and Rap1 (run 2.5 hours 30 mA/gel; transfer 3 hours at constant 380 mA), Myo9b (run 16 hours 30 mA/gel; transfer 6 hours at constant 380 mA). After transfer, traditional Western blotting protocols applied (24).

Kinase assay

In vitro phosphorylation assessment was performed using immunoprecipitated proteins, as described (15). Briefly, proteins were incubated with the catalytic subunit of PKA (P6000S, New England Biolabs) in the presence of 50 mM Tris/HCl pH 7.5, 10 mM MgCl₂ and 50

μM cold ATP mixed with 1 μCi [γ - ^{32}P]ATP (BLU502A100UC, Perkin Elmer) at 30 °C for 90 seconds. The reaction was stopped by addition of sample buffer and boiling and analyzed by SDS-PAGE and blotting followed by autoradiography. Blots were then analysed by Western blotting to verify total protein levels.

Densitometry & Statistical analysis

All Western blots analysed by ECL and x-ray film were exposed for the same length of time on one x-ray film for the same experiment, allowing detection of protein levels to be identical across, for example, IP and total protein levels, providing more accurate interpretations of changes in specific protein levels as ECL detection is semi-quantitative. ECL developed western blots were scanned as 600 dpi greyscale TIFF images using a CanoScan LiDE 90 scanner (Canon, Tokyo, Japan). Densitometry was performed using ImageJ software (25) using whole lane boxed analysis. Western blots analysed using the LI-COR Odyssey scanning system are denoted in the respective figure legends and were analysed using Image Studio software (LI-COR). For platelet experiments ratios of band intensities were calculated and plotted. For transfected cells, calculated ratios were then normalized to controls (set to 1). All statistical analyses were performed using One-Way ANOVA and Bonferroni post-hoc test (Prism 6 software, GraphPad).

Results

PKA/PKG-mediated RhoA regulation may not be due to direct phosphorylation

The ability of cyclic nucleotide signalling to inhibit or reverse RhoA activation has been previously documented in platelet and endothelial cells ((8, 26) and supplementary Fig. 1A). RhoA has been described as the nexus of this mechanism, by being a direct target for PKA and PKG phosphorylation in platelets. This was shown by Western blotting using anti-phospho-RhoA (pS188) antibodies (11, 13). We attempted to replicate these findings by analysing lysates of platelets treated with prostaglandin E1 (PGE₁), an agonist of the PGI₂ receptor, or forskolin, a direct activator of adenylate cyclase. Running samples on high-concentration acrylamide gels (13%) and blotting with anti-pS188-RhoA (Abcam) revealed three bands that increased in intensity in response to activation of cAMP signalling (Fig. 1A, right panel), however, none of these bands ran at the same level as RhoA (Fig. 1A, left panel). PKA activation in the samples was confirmed by detection of phosphorylated serine 7 of Rap1GAP2, an established PKA substrate in platelets (17). The absence of a phospho-RhoA band was confirmed using a second anti-phospho-RhoA antibody from a different manufacturer (Biorbyt, Supplementary Fig. 1B). These data suggested that currently available anti-pS188-RhoA antibodies might either be unspecific or that RhoA might not be phosphorylated in human platelets. To test the ability of anti-pS188-RhoA antibodies to detect RhoA we overexpressed RhoA in HEK293T cells. Following forskolin treatment a faint band of phosphorylated RhoA could be detected (Supplementary Fig. 1C) suggesting that anti-pS188-RhoA antibodies can detect RhoA. Therefore, to verify if RhoA is phosphorylated in platelets we employed Phos-tag gel electrophoresis, a method that does not require phospho-specific antibodies and that has been shown to enable phosphoprotein detection in human platelets

before (15, 16). In brief, the Phos-tag compound allows for efficient separation of phosphorylated and non-phosphorylated protein species which can be detected using total antibodies (24). Platelet-derived RhoA appeared as a single band with no evidence of a phosphorylation-induced band shift following PGE₁ treatment (Fig. 1B). We observed a faint band above RhoA in untreated as well as PGE₁ treated samples. To exclude that this band might represent phosphorylated RhoA we treated samples with λ protein phosphatase (λ PP) before Phos-tag analysis to remove possible phosphate groups. λ PP treatment did not alter band patterns confirming the absence of any RhoA phosphorylation. We also found platelet-derived RhoA appeared as a single band following forskolin treatment and SNP treatment (Supplementary Fig. 1D). To verify Phos-tag gels as an appropriate method for the analysis of small G-protein phosphorylation we assessed Rap1, an established substrate of PKA in platelets (27, 28). Phos-tag gel analysis of PGE₁-treated platelets lead to the appearance of a shifted band confirming Rap1 phosphorylation in platelets (Fig. 1C). These data suggest that RhoA may not be phosphorylated directly by PKA or PKG in human platelets.

PKA and PKG phosphorylate Myo9b S1354, enhancing Myo9b GAP activity

To identify alternative mechanisms that could explain PKA/PKG-induced RhoA inhibition, we searched quantitative platelet phosphoproteomics data of human platelets treated with iloprost, a stable PGI₂ analogue (4, 14), or riociguat, an sGC stimulator ((3) and SG, UW, OP, RPZ, KJ, unpublished), for candidate GAP and GEF proteins of RhoA. Of 20 phosphorylated GAP proteins detected in platelets we excluded proteins not containing PKA/PKG consensus phosphorylation sites (R-R/K-x-pS/pT (29)) and not being RhoA specific according to the literature. This resulted in the identification of Myo9b as a candidate for PKA/PKG phosphorylation. To verify Myo9b as a PKA substrate, we first assessed phosphorylation in a cell free setting. eGFP-tagged Myo9b expressed in HEK293T cells and purified via GFP immunoprecipitation could be phosphorylated by the catalytic subunit of PKA (Fig. 2A and supplementary Fig. 2A). To test phosphorylation of endogenous Myo9b in intact platelets we used Phos-tag gels. In untreated platelets, Myo9b appeared as one band. Incubation with PGE₁ or forskolin led to the appearance of a second band indicative of phosphorylation (Figs. 2B and 2C). We also observed a similar band shift in platelets treated with the NO donor SNP (Supplementary Fig. 2B). These data confirmed Myo9b as a substrate for PKA and PKG phosphorylation in human platelets. Interestingly, platelet activators thrombin and U46619 also induced a band shift (Fig. 2B, second and third lanes), suggestive of cAMP-independent phosphorylation of Myo9b.

Mass spectrometry studies in platelets ((3, 4, 14) and SG, UW, OP, RPZ, KJ, unpublished) suggested serine S1354 (-R-R-T-pS-F) of Myo9b as the main PKA/PKG phosphorylation site. Furthermore, Myo9b S1354 phosphorylation has been detected in other cell types as well (PhosphoSitePlus, (30)). S1354 matches the PKA/PKG consensus sequence and the site is conserved in many species including rat, mouse, dog, and pig as assessed by Clustal Omega alignment (31). To verify S1354 of Myo9b as target for PKA, we performed Phos-tag analysis of eGFP-tagged wildtype and S1354A mutant Myo9b expressed in HEK293T cells. Prior to lysis cells were treated with forskolin to activate endogenous PKA. Forskolin treatment induced a band shift of wildtype Myo9b (Fig. 2D, second lane p2)

compared to control (Fig. 2D, first lane p1). S1354A mutant Myo9b ran slightly lower than wildtype Myo9b suggesting a reduced degree of basal phosphorylation (Fig. 2D, third lane b). Importantly, S1354A mutation abolished the forskolin induced band shift (Fig. 2D, fourth lane b). These results confirm S1354 as a PKA phosphorylation site on Myo9b. The data also indicate that Myo9b might be phosphorylated on other residues that could be dependent on the presence of S1354. Indeed, treatment of lysates of Myo9b expressing cells with λ PP prior to Phos-tag gel analysis lead to a downward shift of the Myo9b band below p1 (Supplementary Fig. 2C).

To examine possible functional consequences of S1354 phosphorylation we measured the GAP activity of Myo9b towards endogenous RhoA using pull-down assays in HEK293T cells. In these experiments the rat ortholog was used which is 84% identical to human Myo9b at the protein level (including the S1354 (S1327 in rat) phosphorylation site (Supplementary Fig. 2D)). As shown in Fig. 2E both wildtype and SA mutant Myo9b expression led to a reduction in RhoA-GTP levels compared to controls. However, mutation of the PKA phosphorylation site of Myo9b caused a less pronounced inhibition of RhoA-GTP (Fig. 2F) suggesting that presence of the phospho-site is required for full GAP activity. These results confirm that Myo9b is a GAP of RhoA. Furthermore, the data indicate that PKA mediated phosphorylation may enhance the GAP activity of Myo9b.

PKA and PKG phosphorylate GEF-H1 on S886 increasing 14-3-3 binding

Previous studies have indicated that cyclic nucleotide pathways can target both GAP as well as GEF proteins of small G-proteins like Rap1 and Rac1 (15, 17). Screening of platelet phospho-proteome data as described above revealed the RhoA-specific GEF GEF-H1 (ARHGEF2) as another potential candidate for PKA/PKG phosphorylation. GEF-H1 has been shown to be phosphorylated by PKA on S886 (-R-R-R-pS-L-) in other cells before (32). In addition, previous data also suggested that phosphorylated S886 might be a binding site for the adapter protein 14-3-3 and 14-3-3 binding has been linked to GEF-H1 inhibition (32). To study the role of GEF-H1 and S886 phosphorylation in platelets, we performed pull-down assays using GST-14-3-3 β in lysates of PGE₁, forskolin or SNP treated platelets. A basal level of interaction between 14-3-3 β and GEF-H1 could be detected in untreated platelets which increased following activation of PKA/PKG (Fig. 3A, upper panel). This increase in binding to 14-3-3 β correlated with an increase in S886 phosphorylation (Fig. 3A, middle panel, and Fig. 3B). To further investigate a possible regulatory role of GEF-H1 and its phosphorylation in platelets we measured effects of known RhoA activators, thrombin and thromboxane A2 in platelets. Treatment of platelets with thrombin or the thromboxane receptor agonist U46619 reduced GEF-H1/14-3-3 β binding and did not induce S886 phosphorylation (Fig. 3C). GEF-H1 is the only Rho-GEF known to be negatively regulated by microtubule binding (33-35). We therefore analysed effects of the microtubule-depolymerizing agent nocodazole on RhoA-GTP levels in platelets. Nocodazole treatment strongly increased RhoA-GTP levels compared to controls (Fig. 3D, E), confirming an important role of GEF-H1 for RhoA activation in platelets. The well-established ability of cyclic nucleotide pathways to inhibit RhoA-GTP formation correlated with GEF-H1 S886 phosphorylation and was not affected by nocodazole treatment (Fig. 3D, E). These results suggest that GEF-H1 might be another protein involved in the

inhibition of RhoA by cyclic nucleotide pathways in platelets in addition to Myo9b. GEF-H1 regulation involves the phosphorylation of GEF-H1 on S886 and 14-3-3 binding.

Discussion

Carefully controlled cycling of RhoA between active and inactive conformations represents a key signaling principle in many cells. In the present study we describe Myo9b and GEF-H1 as novel RhoA regulators and targets for endothelium and cyclic nucleotide dependent RhoA inhibition in platelets (Fig. 4).

RhoA phosphorylation at S188 has previously been suggested as a mechanism of RhoA regulation by cyclic nucleotides in different cell types including platelets (10-13, 36, 37). Platelet experiments were based on standard immunoblotting methods using phospho-specific antibodies. However, our studies indicate that the detection of RhoA S188 phosphorylation with phospho-specific antibodies is not reliable and that the signals obtained might derive from other proteins. Using antibodies from two different suppliers we were not able to detect any evidence of RhoA phosphorylation after platelet treatment with comparable concentrations of cAMP/PKA agonists as described before (11, 13). Instead, antibodies cross-reacted with proteins of similar but not identical apparent molecular weight as RhoA. These bands could potentially have been mistaken for RhoA in previous studies due to the use of lower percentage SDS-PAA gels (10% in Atkinson et al. (13) compared to 13% in our study) which are less effective in resolving differences between small proteins. Unfortunately the phospho-RhoA S188 antibody used before ((11-13) from Santa Cruz Biotechnology) is no longer available and it cannot be ruled out that it might have been more specific compared to the Abcam and Biorbyt antibodies used here. Nonetheless we were able to confirm that the Abcam antibody (shown in Fig. 1A) is indeed able to detect overexpressed RhoA (Supplementary Fig. 1C). Of note, the constitutive posttranslational geranylgeranylation of RhoA at C190 required for cell membrane localization of RhoA has been shown to reduce the binding of phospho-RhoA S188 antibodies (10), which could contribute to detection problems. However, using Phos-tag gels, a method independent of phospho-specific antibodies, we were also not able to detect any RhoA phosphorylation in response to PKA activation in human platelets. As a positive control we used Rap1, which is a known more slowly phosphorylated PKA substrate (38). However, conditions that facilitated Rap1 phosphorylation did not induce RhoA phosphorylation. We conclude that direct S188 phosphorylation is unlikely to mediate PKA/PKG induced RhoA inhibition in platelets. Interestingly, endogenous RhoA phosphorylation could not be verified in studies of other cell types before. Bolz et al. reported that PKG-induced RhoA inhibition was independent of RhoA phosphorylation in resistance arteries (39), and Oishi et al. showed that RhoGDI phosphorylation was involved in PKA-mediated RhoA inhibition in cardiac fibroblasts instead of RhoA phosphorylation (40).

Our study indicates that the RhoA GAP and GEF proteins Myo9b and GEF-H1 might be the actual PKA/PKG targets involved in RhoA inhibition. Both proteins have recently been confirmed to be RhoA specific (41). Myo9b is also a myosin motor protein that can move along actin filaments towards their plus-end (42). The motor domain is linked to a GAP domain which is thought to provide local control of RhoA at sites of actin polymerization (23). Myo9b has been implicated in lamellipodia formation and cell migration in macrophages, T-cells, and

epithelial cells (43-45). These Myo9b functions were associated with a regulation of RhoA-GTP levels. Myo9b has not previously been described in platelets nor has its phosphorylation by cyclic nucleotide-dependent kinases. We mapped Myo9b phosphorylation to a highly conserved S1354 site localized between the N-terminal myosin motor and IQ or myosin light chain binding domains (aa146-953, aa957-1053) and the C-terminal GAP domain (aa1703-1888). S1354 lies in the centre of a large uncharacterized region between amino acids 1100 to 1500 scoring high for intrinsic protein disorder (46). Disordered regions are increasingly recognized as common targets for phosphorylation in many proteins (47). Our studies indicate that S1354 phosphorylation might enhance the GAP activity of Myo9b leading to reduced RhoA-GTP levels. Thus, Myo9b phosphorylation could contribute to local cyclic nucleotide-mediated control of RhoA and the actin/myosin cytoskeleton in platelets. Previous studies of other small G-proteins like Rap1, Rac1, and Gq indicate that GAP regulation might be a common mechanism of cyclic nucleotide dependent control of platelets (15-17, 48, 49). We also observed agonist induced phosphorylation of Myo9b, suggestive of cAMP-independent PKA-mediated phosphorylation, previously proposed as an inhibitory feedback mechanism during thrombin- and collagen-induced platelet activation (50).

GEF-H1 has been shown to be expressed in platelets before (51) and it is known to regulate endomitosis of megakaryocytes (52). In the present study, we show that PKA and PKG phosphorylate GEF-H1 on S886 in human platelets leading to an increase in 14-3-3 β interaction. PKA induced S886 phosphorylation has been described (32) and also other kinases like p21-activated kinase 1 or microtubule affinity-regulating kinase 2 (Par-1b) can phosphorylate S886 of GEF-H1 in cells other than platelets (34, 53). These studies have also indicated that S886 phosphorylation and 14-3-3 binding contribute to inhibition of GEF-H1 activity, however, the phosphorylation of additional sites might be necessary for full GEF-H1 inhibition (54). In contrast, dephosphorylation and loss of 14-3-3 might play a role in GEF-H1 activation by thrombin (55). Our data support this concept showing that thrombin and thromboxane A2 reduce the interaction of GEF-H1 with 14-3-3. Thus 14-3-3 binding might constitute a switch used by cyclic nucleotide pathways to block GEF-H1 mediated RhoA activation, whereas platelet activators detach 14-3-3 from GEF-H1 to stimulate RhoA. A similar, although reverse, role of 14-3-3 has been described previously for RGS18, a GAP of Gq. Cyclic nucleotide inhibitory pathways detach 14-3-3 from RGS18 to activate it and to block Gq function, whereas platelet activators use 14-3-3 binding to stop RGS18 from turning off Gq signalling (1, 16, 48). The inactivation of GEF-H1 by 14-3-3 is linked to microtubule binding of the N-terminal domain of GEF-H1 (21) and GEF-H1 is the only GEF reported to localize at microtubules (35). Therefore, our finding that nocodazole-induced disruption of microtubules increases RhoA-GTP levels corroborate an important role for GEF-H1 in RhoA regulation in platelets. PKA-mediated GEF-H1 S886 phosphorylation and RhoA inhibition were not affected by the presence or absence of microtubules suggesting that cyclic nucleotide pathways might be able to inhibit GEF-H1 independent of its subcellular localisation.

In conclusion we have identified new mechanisms of cyclic nucleotide dependent RhoA inhibition in platelets. Recently, Myo9b and GEF-H1 were shown to form a network with RhoA and actin filaments generating dynamic patterns of subcellular contractility (56). Initial experiments in our group indicate that Myo9b and GEF-H1 bind to each other independent of S1354 phosphorylation or microtubule integrity (Supplementary Fig. 3B). It will be interesting

to investigate how PKA and PKG mediated control of RhoA is coordinated at the level of Myo9b and GEF-H1 and ultimately at the wider level of the many hundred other substrates phosphorylated in platelets simultaneously (4).

Acknowledgements

We thank Martin Bähler for providing the Myo9b rat orthologue plasmid and Harry Mellor for the GST-Rhotekin-RBD plasmid. We also thank all blood donors for contributing to this research. Funding was provided by UCD School of Medicine, University College Dublin. SG was supported by a grant from the Russian Foundation For Basic Research (RFBR # 17-00-00141 (17-00-00139)). KJ, OP and RZ were supported by the German Research Foundation (DFG), ZA 639/4-1 and JU 2735/2-1.

Conflicts of Interest

The authors declare that they have no actual or potential conflicts of interest with the contents of this article.

Author Contribution

SC and AS designed the research, performed experiments, and wrote the paper. ZN, AB, AvK, SG, UW, OP, RZ and KJ performed phosphorylation site analyses and contributed to research design and paper writing.

References

1. Nagy Z, Smolenski A. Cyclic nucleotide-dependent inhibitory signaling interweaves with activating pathways to determine platelet responses. *Research and practice in thrombosis and haemostasis*. 2018;2(3):558-71.
2. Raslan Z, Naseem Khalid M. The control of blood platelets by cAMP signalling. *Biochemical Society Transactions*. 2014;42(2):289-94.
3. Makhoul S, Walter E, Pagel O, Walter U, Sickmann A, Gambaryan S, et al. Effects of the NO/soluble guanylate cyclase/cGMP system on the functions of human platelets. *Nitric Oxide*. 2018;76:71-80.
4. Beck F, Geiger J, Gambaryan S, Veit J, Vaudel M, Nollau P, et al. Time-resolved characterization of cAMP/PKA-dependent signaling reveals that platelet inhibition is a concerted process involving multiple signaling pathways. *Blood*. 2014;123(5):e1-e10.
5. Klages B, Brandt U, Simon MI, Schultz G, Offermanns S. Activation of G12/G13 results in shape change and Rho/Rho-kinase-mediated myosin light chain phosphorylation in mouse platelets. *The Journal of cell biology*. 1999;144(4):745-54.
6. Pleines I, Hagedorn I, Gupta S, May F, Chakarova L, van Hengel J, et al. Megakaryocyte-specific RhoA deficiency causes macrothrombocytopenia and defective platelet activation in hemostasis and thrombosis. *Blood*. 2012;119(4):1054-63.
7. Aslan JE, McCarty OJ. Rho GTPases in platelet function. *Journal of thrombosis and haemostasis : JTH*. 2013;11(1):35-46.
8. Gratacap M-P, Payrastré B, Nieswandt B, Offermanns S. Differential Regulation of Rho and Rac through Heterotrimeric G-proteins and Cyclic Nucleotides. *Journal of Biological Chemistry*. 2001;276(51):47906-13.
9. Suzuki A, Shin J-W, Wang Y, Min SH, Poncz M, Choi JK, et al. RhoA Is Essential for Maintaining Normal Megakaryocyte Ploidy and Platelet Generation. *PLOS ONE*. 2013;8(7):e69315.
10. Ellerbroek SM, Wennerberg K, Burridge K. Serine Phosphorylation Negatively Regulates RhoA in Vivo. *Journal of Biological Chemistry*. 2003;278(21):19023-31.
11. Aburima A, Wraith KS, Raslan Z, Law R, Magwenzi S, Naseem KM. cAMP signaling regulates platelet myosin light chain (MLC) phosphorylation and shape change through targeting the RhoA-Rho kinase-MLC phosphatase signaling pathway. *Blood*. 2013;122(20):3533-45.
12. Aburima A, Walladbeji K, Wake JD, Naseem KM. cGMP signaling inhibits platelet shape change through regulation of the RhoA-Rho Kinase-MLC phosphatase signaling pathway. *Journal of Thrombosis and Haemostasis*. 2017;15(8):1668-78.
13. Atkinson L, Yusuf MZ, Aburima A, Ahmed Y, Thomas SG, Naseem KM, et al. Reversal of stress fibre formation by Nitric Oxide mediated RhoA inhibition leads to reduction in the height of preformed thrombi. *Scientific Reports*. 2018;8(1):8:3032.
14. Beck F, Geiger J, Gambaryan S, Solari FA, Dell'Aica M, Loroach S, et al. Temporal quantitative phosphoproteomics of ADP stimulation reveals novel central nodes in platelet activation and inhibition. *Blood*. 2017;129(2):e1-e12.
15. Nagy Z, Wynne K, von Kriegsheim A, Gambaryan S, Smolenski A. Cyclic Nucleotide-dependent Protein Kinases Target ARHGAP17 and ARHGAP6 Complexes in Platelets. *The Journal of biological chemistry*. 2015;290(50):29974-83.
16. Gegenbauer K, Elia G, Blanco-Fernandez A, Smolenski A. Regulator of G-protein signaling 18 integrates activating and inhibitory signaling in platelets. *Blood*. 2012;119(16):3799-807.
17. Hoffmeister M, Riha P, Neumüller O, Danielewski O, Schultess J, Smolenski AP. Cyclic Nucleotide-dependent Protein Kinases Inhibit Binding of 14-3-3 to the GTPase-activating Protein Rap1GAP2 in Platelets. *Journal of Biological Chemistry*. 2008;283(4):2297-306.
18. Elvers M. RhoGAPs and Rho-GTPases in platelets. *Hamostaseologie*. 2015;36(03):168-77.
19. Goggs R, Williams CM, Mellor H, Poole AW. Platelet Rho GTPases—a focus on novel players, roles and relationships. *Biochem J*. 2015;466(3):431-42.
20. Müller RT, Honnert U, Reinhard J, Bähler M. The rat myosin myr 5 is a GTPase-activating protein for Rho in vivo: essential role of arginine 1695. *Molecular biology of the cell*. 1997;8(10):2039-53.
21. Krendel M, Zenke FT, Bokoch GM. Nucleotide exchange factor GEF-H1 mediates cross-talk between microtubules and the actin cytoskeleton. *Nature cell biology*. 2002;4:294-301.

22. von Thun A, Preisinger C, Rath O, Schwarz JP, Ward C, Monsefi N, et al. Extracellular signal-regulated kinase regulates RhoA activation and tumor cell plasticity by inhibiting guanine exchange factor H1 activity. *Molecular and cellular biology*. 2013;33(22):4526-37.
23. van den Boom F, Düsselmann H, Uhlenbrock K, Abouhamed M, Bähler M. The Myosin IXb Motor Activity Targets the Myosin IXb RhoGAP Domain as Cargo to Sites of Actin Polymerization. *Molecular Biology of the Cell*. 2007;18(4):1507-18.
24. Nagy Z, Comer S, Smolenski A. Analysis of Protein Phosphorylation Using Phos-Tag Gels. *Current Protocols in Protein Science*. 2018;93(1):e64.
25. Schneider CA, Rasband WS, Eliceiri KW. NIH Image to ImageJ: 25 years of image analysis. *Nature methods*. 2012;9(7):671-5.
26. Qiao J, Huang F, Lum H. PKA inhibits RhoA activation: a protection mechanism against endothelial barrier dysfunction. *American journal of physiology Lung cellular and molecular physiology*. 2003;284(6):L972-80.
27. Altschuler D, Lapetina EG. Mutational analysis of the cAMP-dependent protein kinase-mediated phosphorylation site of Rap1b. *Journal of Biological Chemistry*. 1993;268(10):7527-31.
28. Takahashi M, Li Y, Dillon TJ, Stork PJS. Phosphorylation of Rap1 by cAMP-dependent Protein Kinase (PKA) Creates a Binding Site for KSR to Sustain ERK Activation by cAMP. *The Journal of biological chemistry*. 2017;292(4):1449-61.
29. Kennelly PJ, Krebs EG. Consensus sequences as substrate specificity determinants for protein kinases and protein phosphatases. *Journal of Biological Chemistry*. 1991;266(24):15555-8.
30. Hornbeck PV, Zhang B, Murray B, Kornhauser JM, Latham V, Skrzypek E. PhosphoSitePlus, 2014: mutations, PTMs and recalibrations. *Nucleic acids research*. 2015;43(Database issue):D512-D20.
31. Sievers F, Wilm A, Dineen D, Gibson TJ, Karplus K, Li W, et al. Fast, scalable generation of high-quality protein multiple sequence alignments using Clustal Omega. *Molecular systems biology*. 2011;7:539.
32. Meiri D, Greeve MA, Brunet A, Finan D, Wells CD, LaRose J, et al. Modulation of Rho guanine exchange factor Lfc activity by protein kinase A-mediated phosphorylation. *Molecular and cellular biology*. 2009;29(21):5963-73.
33. Chang Y-C, Nalbant P, Birkenfeld J, Chang Z-F, Bokoch GM. GEF-H1 couples nocodazole-induced microtubule disassembly to cell contractility via RhoA. *Molecular biology of the cell*. 2008;19(5):2147-53.
34. Zenke FT, Krendel M, DerMardirossian C, King CC, Bohl BP, Bokoch GM. p21-activated Kinase 1 Phosphorylates and Regulates 14-3-3 Binding to GEF-H1, a Microtubule-localized Rho Exchange Factor. *Journal of Biological Chemistry*. 2004;279(18):18392-400.
35. Azoitei ML, Noh J, Marston DJ, Roudot P, Marshall CB, Daugird TA, et al. Spatiotemporal dynamics of GEF-H1 activation controlled by microtubule- and Src-mediated pathways. *Journal of Cell Biology*. 2019;218(9):3077-97.
36. Sauzeau V, Le Jeune H, Cario-Toumaniantz C, Smolenski A, Lohmann SM, Bertoglio J, et al. Cyclic GMP-dependent Protein Kinase Signaling Pathway Inhibits RhoA-induced Ca²⁺ Sensitization of Contraction in Vascular Smooth Muscle. *Journal of Biological Chemistry*. 2000;275(28):21722-9.
37. Sawada N, Itoh H, Yamashita J, Doi K, Inoue M, Masatsugu K, et al. cGMP-Dependent Protein Kinase Phosphorylates and Inactivates RhoA. *Biochemical and biophysical research communications*. 2001;280(3):798-805.
38. Smolenski A. Novel roles of cAMP/cGMP-dependent signaling in platelets. *Journal of thrombosis and haemostasis : JTH*. 2012;10(2):167-76.
39. Bolz S-S, Vogel L, Sollinger D, Derwand R, de Wit C, Loirand G, et al. Nitric Oxide-Induced Decrease in Calcium Sensitivity of Resistance Arteries Is Attributable to Activation of the Myosin Light Chain Phosphatase and Antagonized by the RhoA/Rho Kinase Pathway. *Circulation*. 2003;107(24):3081-7.
40. Oishi A, Makita N, Sato J, Iiri T. Regulation of RhoA Signaling by the cAMP-dependent Phosphorylation of RhoGDI α . *Journal of Biological Chemistry*. 2012;287(46):38705-15.
41. Bagci H, Sriskandarajah N, Robert A, Boulais J, Elkholi IE, Tran V, et al. Mapping the proximity interaction network of the Rho-family GTPases reveals signalling pathways and regulatory mechanisms. *Nature cell biology*. 2020;22(1):120-34.

42. Liao W, Elfrink K, Bähler M. Head of Myosin IX Binds Calmodulin and Moves Processively toward the Plus-end of Actin Filaments. *Journal of Biological Chemistry*. 2010;285(32):24933-42.
43. Hanley PJ, Xu Y, Kronlage M, Grobe K, Schön P, Song J, et al. Motorized RhoGAP myosin IXb (Myo9b) controls cell shape and motility. *Proceedings of the National Academy of Sciences*. 2010;107(27):12145-50.
44. Moalli F, Ficht X, Germann P, Vladymyrov M, Stolp B, de Vries I, et al. The Rho regulator Myosin IXb enables nonlymphoid tissue seeding of protective CD8(+) T cells. *The Journal of experimental medicine*. 2018;215(7):1869-90.
45. Chandhoke SK, Mooseker MS. A role for myosin IXb, a motor–RhoGAP chimera, in epithelial wound healing and tight junction regulation. *Molecular Biology of the Cell*. 2012;23(13):2468-80.
46. Mészáros B, Erdos G, Dosztányi Z. IUPred2A: context-dependent prediction of protein disorder as a function of redox state and protein binding. *Nucleic acids research*. 2018;46(W1):W329-W37.
47. Bah A, Forman-Kay JD. Modulation of Intrinsically Disordered Protein Function by Post-translational Modifications. *Journal of Biological Chemistry*. 2016;291(13):6696-705.
48. Gegenbauer K, Nagy Z, Smolenski A. Cyclic nucleotide dependent dephosphorylation of regulator of G-protein signaling 18 in human platelets. *PLoS one*. 2013;8(11):e80251-e.
49. Lévy M, Settleman J, Ligeti E. Regulation of the substrate preference of p190RhoGAP by protein kinase C-mediated phosphorylation of a phospholipid binding site. *Biochemistry*. 2009;48(36):8615-23.
50. Gambaryan S, Kobsar A, Rukoyatkina N, Herterich S, Geiger J, Smolenski A, et al. Thrombin and collagen induce a feedback inhibitory signaling pathway in platelets involving dissociation of the catalytic subunit of protein kinase A from an NFkappaB-IkappaB complex. *The Journal of biological chemistry*. 2010;285(24):18352-63.
51. Aslan JE, Baker SM, Loren CP, Haley KM, Itakura A, Pang J, et al. The PAK system links Rho GTPase signaling to thrombin-mediated platelet activation. *American journal of physiology Cell physiology*. 2013;305(5):C519-28.
52. Gao Y, Smith E, Ker E, Campbell P, Cheng E-c, Zou S, et al. Role of RhoA-specific guanine exchange factors in regulation of endomitosis in megakaryocytes. *Developmental cell*. 2012;22(3):573-84.
53. Yamahashi Y, Saito Y, Murata-Kamiya N, Hatakeyama M. Polarity-regulating kinase partitioning-defective 1b (PAR1b) phosphorylates guanine nucleotide exchange factor H1 (GEF-H1) to regulate RhoA-dependent actin cytoskeletal reorganization. *The Journal of biological chemistry*. 2011;286(52):44576-84.
54. Birkenfeld J, Nalbant P, Bohl BP, Pertz O, Hahn KM, Bokoch GM. GEF-H1 modulates localized RhoA activation during cytokinesis under the control of mitotic kinases. *Developmental cell*. 2007;12(5):699-712.
55. Meiri D, Marshall CB, Mokady D, LaRose J, Mullin M, Gingras A-C, et al. Mechanistic insight into GPCR-mediated activation of the microtubule-associated RhoA exchange factor GEF-H1. *Nature Communications*. 2014;5:e4857.
56. Graessl M, Koch J, Calderon A, Kamps D, Banerjee S, Mazel T, et al. An excitable Rho GTPase signaling network generates dynamic subcellular contraction patterns. *The Journal of Cell Biology*. 2017;216(12):4271-85.

Figure legends

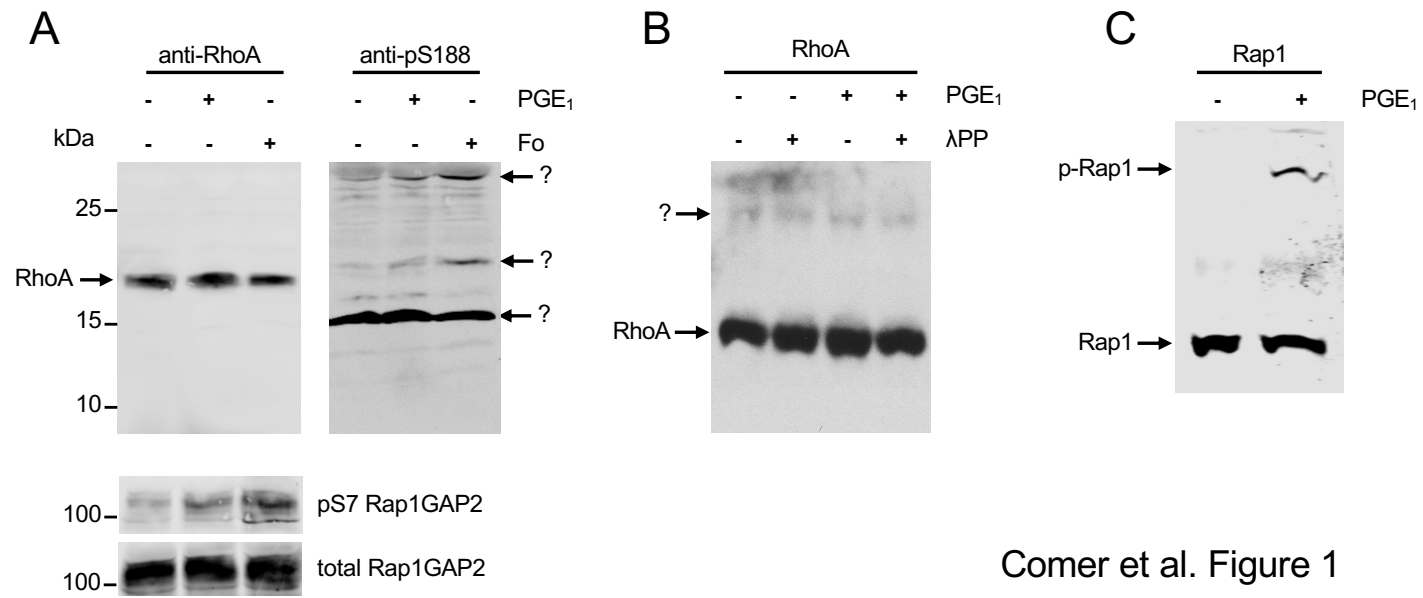
FIGURE 1. RhoA may not be phosphorylated in human platelets. (A) Washed human platelets were incubated with or without PGE₁ (50 nM, 30 sec) or forskolin (10 μM, 10 min) and lysed. SDS-PAGE was performed using 13% acrylamide gels followed by Western blotting and detection using the LI-COR Odyssey scanning system. Membranes were cut, incubated with anti-RhoA or anti-RhoA pS188 antibodies (as highlighted) and realigned for detection. Appearing bands representing RhoA and an unknown protein of higher molecular weight, detected by the anti-RhoA pS188 antibody, are indicated by arrows. RhoA and two unknown proteins detected by the anti-RhoA pS188 antibody are indicated by arrows. Rap1GAP2 S7 was used as a PKA phosphorylation control and detection was performed with a phospho-antibody against pS7 and a Rap1GAP2 total antibody. (B) Washed human platelets were incubated with or without PGE₁ (0.5 μM, 30 sec) and lysed. Platelet lysates were then incubated without or with λ protein phosphatase (λPP) for 60 min at 30°C. Aliquots of samples were subjected to Phos-tag PAGE followed by immunoblotting using an anti-RhoA antibody. A band of unknown identity above RhoA is indicated by an arrow. (C) Washed human platelets were incubated with or without PGE₁ (0.5 μM, 30 sec) and lysed. Aliquots of samples were subjected to Phos-tag PAGE followed by immunoblotting using an anti-Rap1 antibody and Western blotting and detection using the LI-COR Odyssey scanning system. Non-phosphorylated Rap1 and phosphorylated Rap1 (p-Rap1) are denoted by arrows. Data are representative of three independent experiments (A, B, C).

FIGURE 2. Cyclic nucleotide-dependent kinases phosphorylate Myo9b on S1354, enhancing its GAP activity. (A) eGFP-Myo9b was expressed in HEK293T cells, immunoprecipitated and incubated with purified catalytic subunit of PKA (PKA-Cα) in the presence of [γ -³²P]ATP for 90 sec. Samples were subjected to SDS PAGE and blotting. Radiolabelled Myo9b was detected by autoradiography (upper panel) and total Myo9b levels were determined using anti-GFP antibody (lower panel). This experiment was performed once. (B) Washed human platelets were incubated with or without thrombin (0.1 U/ml, 1 min), U46619 (1 μM, 1 min), PGE₁ (0.5 μM, 30 sec) or forskolin (10 μM, 10 min) and lysed. Aliquots of samples were analysed by Phos-tag PAGE followed by immunoblotting using an anti-Myo9b antibody. Basal (p1) and phosphorylated Myo9b (p2) are denoted by arrows. Data are representative of two (thrombin and U46619) or four (PGE₁ and forskolin) independent experiments. (C) Blots of experiments shown in B (PGE₁ and forskolin) were analysed by densitometry and the ratios of phosphorylated (p2) versus non-phosphorylated (p1) Myo9b were calculated. Data of four independent experiments are expressed as means ± SD. Statistical significance of differences between PGE₁ and forskolin treatments and control was determined by One-Way ANOVA and Bonferroni post-test (* $p < 0.01$; ** $p < 0.001$). (D) HEK293T cells expressing Myo9b-WT or S1354A mutant were incubated without or with forskolin (10 μM, 10 min) and lysed. Aliquots of samples were subjected to Phos-tag PAGE followed by immunoblotting using anti-GFP antibody. Appearing Myo9b-WT bands were labelled as p1 (without forskolin) or p2 (with forskolin) and the trailing edge of the WT phospho-bands are demarcated by dotted lines to highlight the PKA-induced band shift. The S1354A band is labelled as b. Data are representative of 4 independent experiments. (E) HEK293T cells were transfected with Myo9b WT or SA and endogenous levels of RhoA-GTP were analysed by pull-down assay followed by SDS-PAGE and Western blotting. Anti-RhoA antibody was used to determine RhoA-GTP (upper panel) and total RhoA levels (middle panel) and anti-GFP antibody was used to determine total Myo9b levels (bottom panel). (F) Blots of experiments shown in A were analysed by densitometry and ratios of RhoA-GTP versus total RhoA were normalized to non-transfected controls (not shown). Data of five independent experiments are expressed as means ± SD. Statistical significance of relative RhoA-GTP levels in relation to the control was determined using One-Way ANOVA with a Bonferroni post-test (* $p < 0.01$).

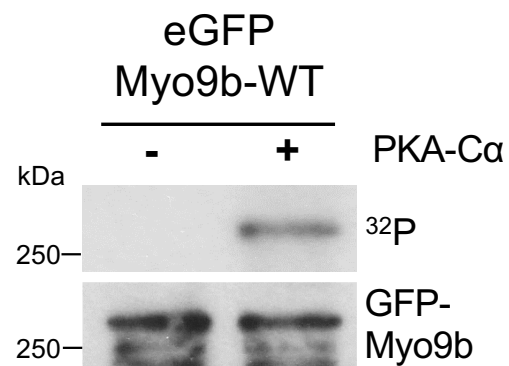
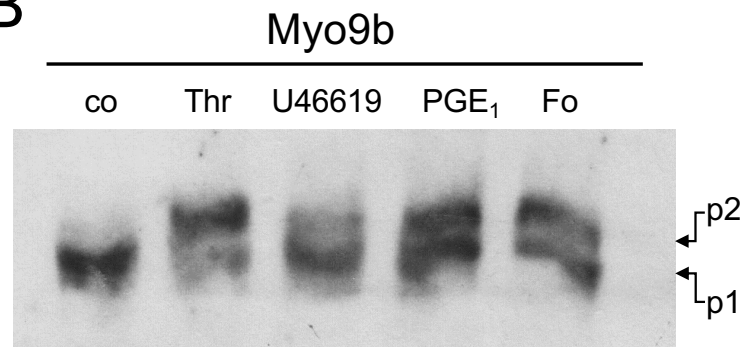
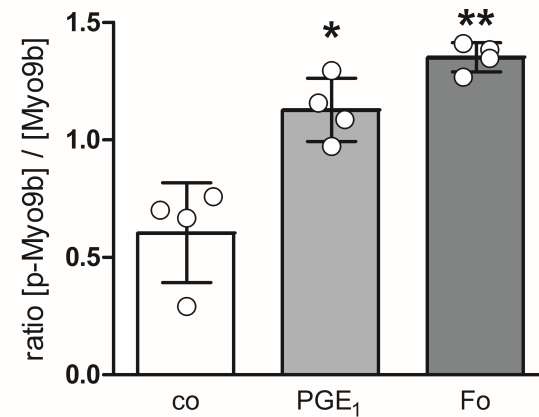
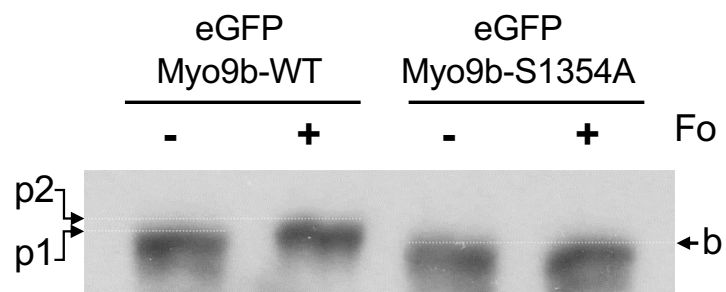
FIGURE 3. GEF-H1 S886 phosphorylation by cyclic nucleotide-dependent kinases increases 14-3-3 binding. (A) Washed human platelets were incubated with PGE₁ (0.5 μM, 30 sec), forskolin (10 μM, 10 min) or SNP (10 μM, 10 min), lysed and subjected to pull-down assays using GST-14-3-3β. As a control, a separate untreated platelet lysate was subjected to a pull-down assay using GST alone

(Supplementary Fig. 3A). Precipitated, (14-3-3 β bound, top panel), total (lower panel) and phosphorylated GEF-H1 (middle panel) were detected by Western blotting. **(B)** Blots of experiments shown in *A* were analysed by densitometry. Ratios of 14-3-3 β bound versus total GEF-H1 and phosphorylated versus non-phosphorylated GEF-H1 were calculated. Data of four independent experiments are expressed as means \pm SD. Statistical significance of differences between treatments and controls was determined by One-Way ANOVA and Bonferroni post-test (14-3-3 β /GEF-H1 interaction; * $p < 0.001$, ** $p < 0.0001$). (GEF-H1 S886 phosphorylation; # $p < 0.0001$). **(C)** Washed human platelets were incubated with or without thrombin (0.1 U/ml, 1 min) or U46619 (1 μ M, 1 min), lysed and subjected to pull-down assays using GST-14-3-3 β . Precipitated, (14-3-3 β bound, top panel), total (lower panel) and phosphorylated GEF-H1 (middle panel) were detected by Western blotting. Data representative of two independent experiments. **(D)** Washed human platelets were incubated with PGE₁ (0.5 μ M, 30 sec) or nocodazole (10 μ M, 1 min) or preincubated with PGE₁ or nocodazole. For preincubated platelets, the order of treatment is indicated by +1 (added first) or +2 (added second). Platelets were lysed, and pull-down assays were performed using GST-RBD followed by Western blotting using anti-RhoA antibody to detect RhoA-GTP levels (top panel). Aliquots of platelet lysate were analysed using anti-RhoA (second panel), anti-GEF-H1 pS886 (third panel) and anti-GEF-H1 (bottom panel). **(E)** Blots of experiments shown in *C* were analysed by densitometry. Ratios of RhoA-GTP versus total RhoA and phosphorylated versus non-phosphorylated GEF-H1 were calculated. Data of three independent experiments are expressed as means \pm SD. Statistical significance of differences between treatments and controls was determined by One-Way ANOVA and Bonferroni post-test. RhoA-GTP; control vs PGE₁ (* $p < 0.001$), control vs nocodazole (** $p < 0.0001$), nocodazole vs PGE₁/Noco and nocodazole vs Noco/PGE₁ (# $p < 0.0001$).

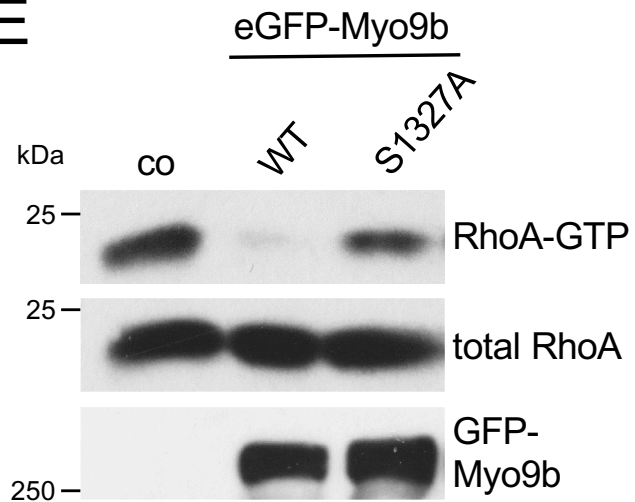
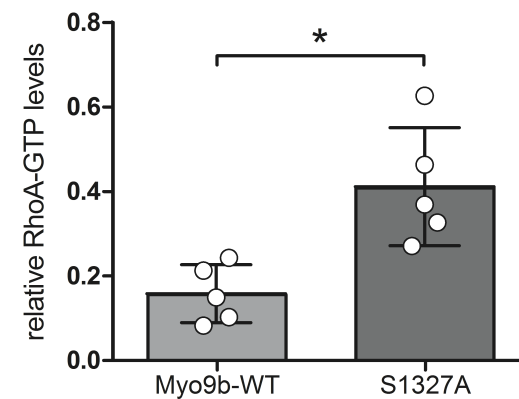
FIGURE 4. Model of RhoA regulation by cyclic nucleotide-dependent protein kinases in human platelets. Endothelium derived PGI₂ and NO inhibit RhoA-GTP formation via stimulation of cyclic nucleotide signalling. PGI₂ binds to the Gs-coupled IP receptor leading to adenylate cyclase (AC) stimulation, cAMP synthesis, and PKA activation. NO stimulates soluble guanylate cyclase (sGC), cGMP synthesis, and PKG activation. PKA and PKG phosphorylate the RhoA-specific GAP, Myo9b, at S1354 resulting in an increase in Myo9b GAP activity and reduction in RhoA-GTP levels. PKA and PKG also phosphorylate GEF-H1, a RhoA-specific GEF, at S886 leading to enhanced 14-3-3 interaction and sequestration of GEF-H1 to platelet microtubules, resulting in a decrease in GEF-H1 GEF activity contributing to a reduction in RhoA-GTP levels. Image created with *BioRender.com*.

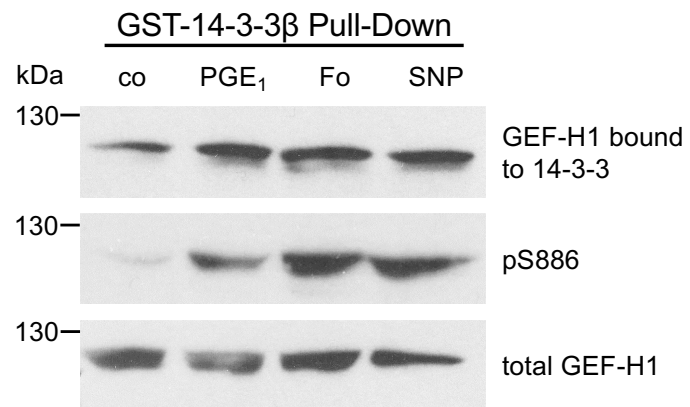
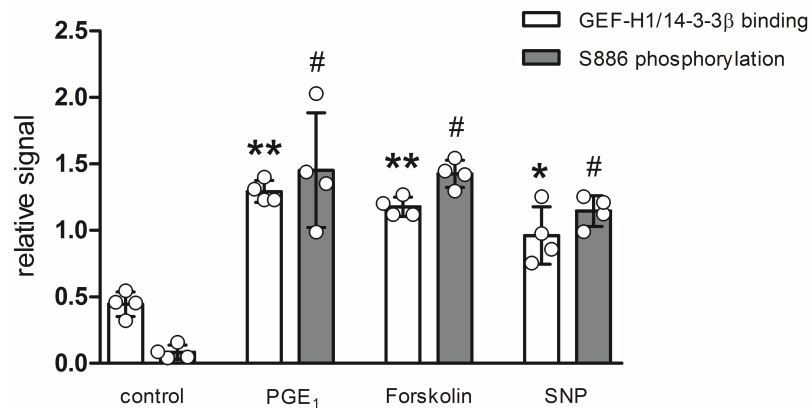
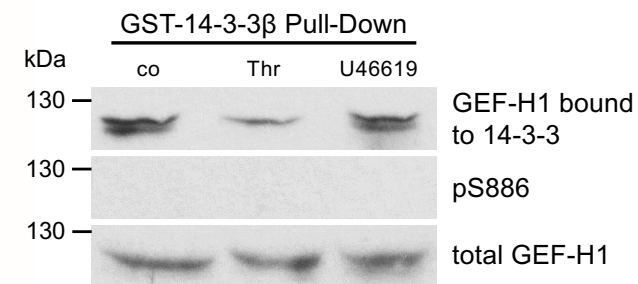
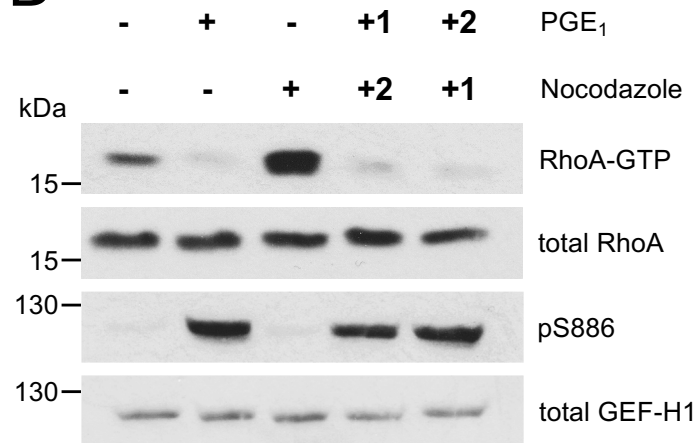
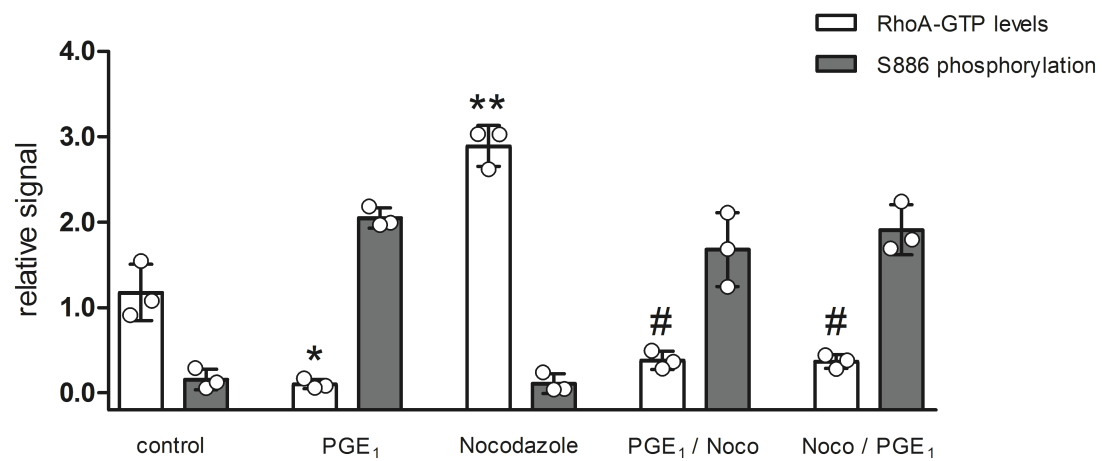


Comer et al. Figure 1

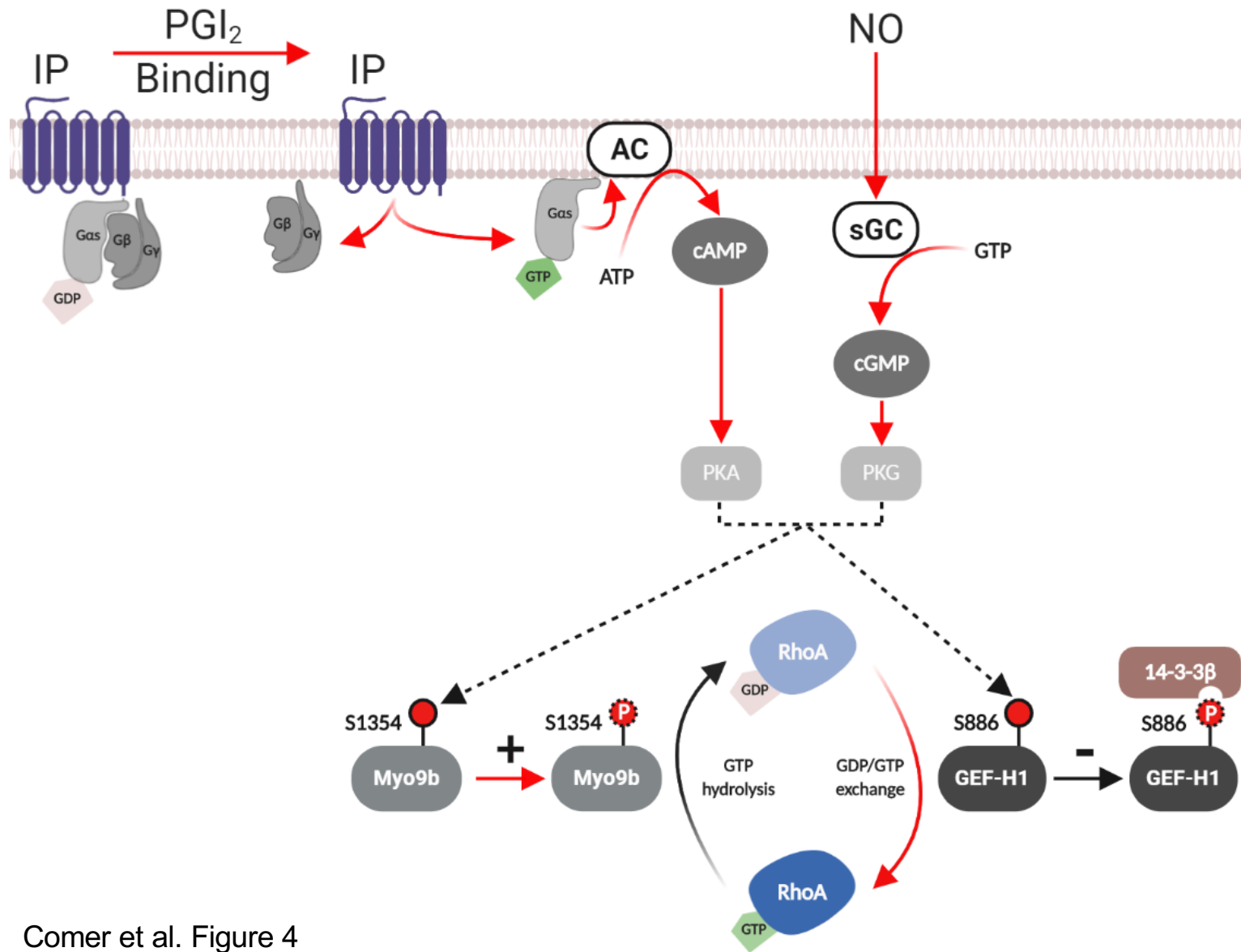
A**B****C****D**

Comer et al. Figure 2

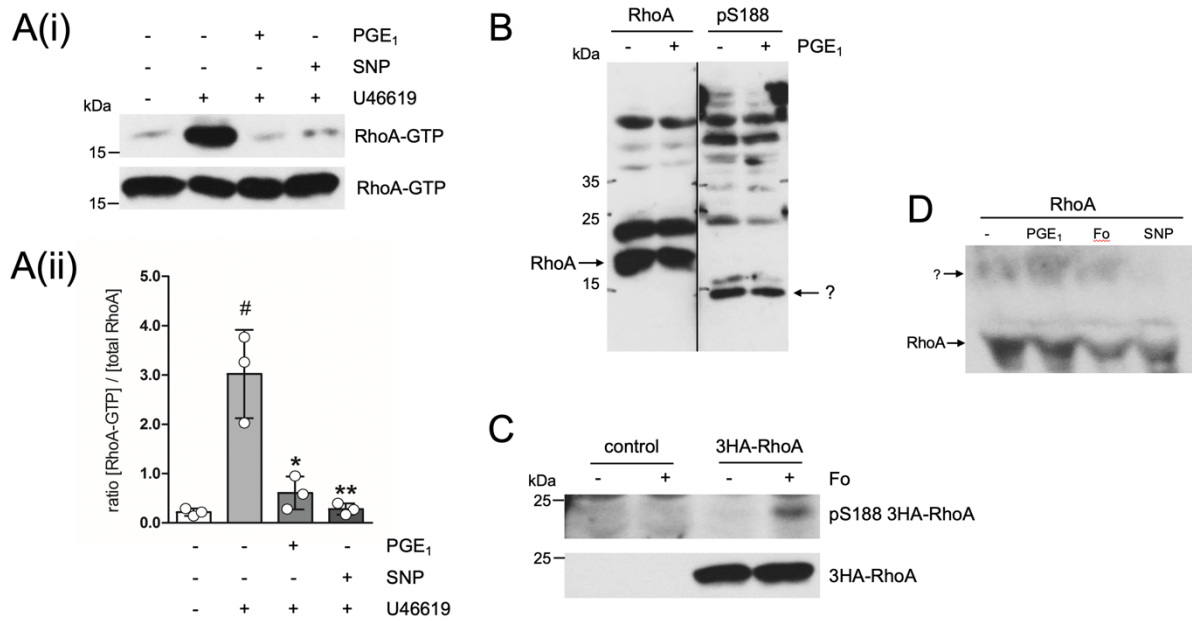
E**F**

A**B****C****D****E**

Comer et al. Figure 3

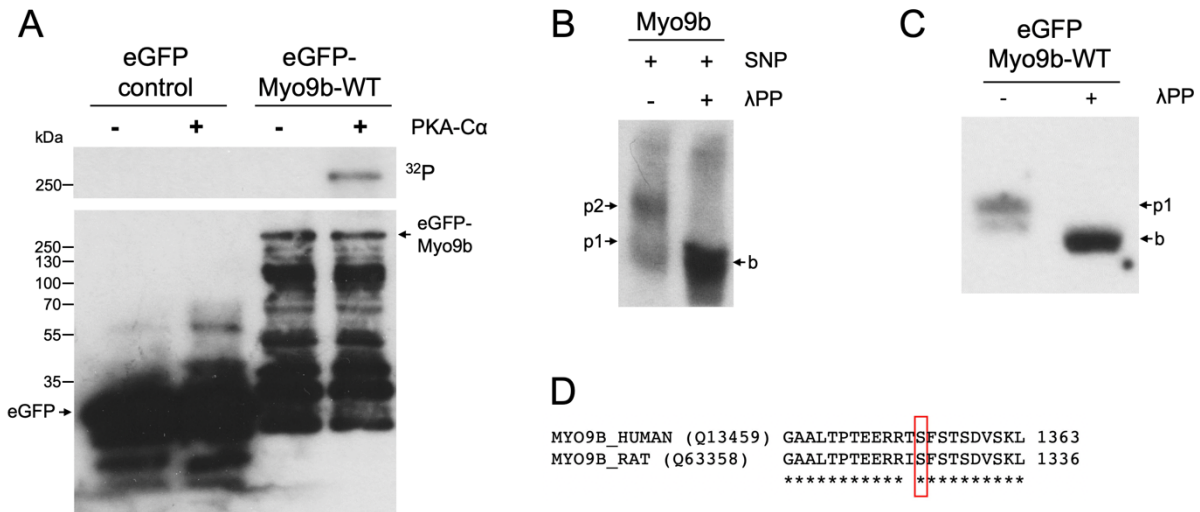


Comer et al. Figure 4



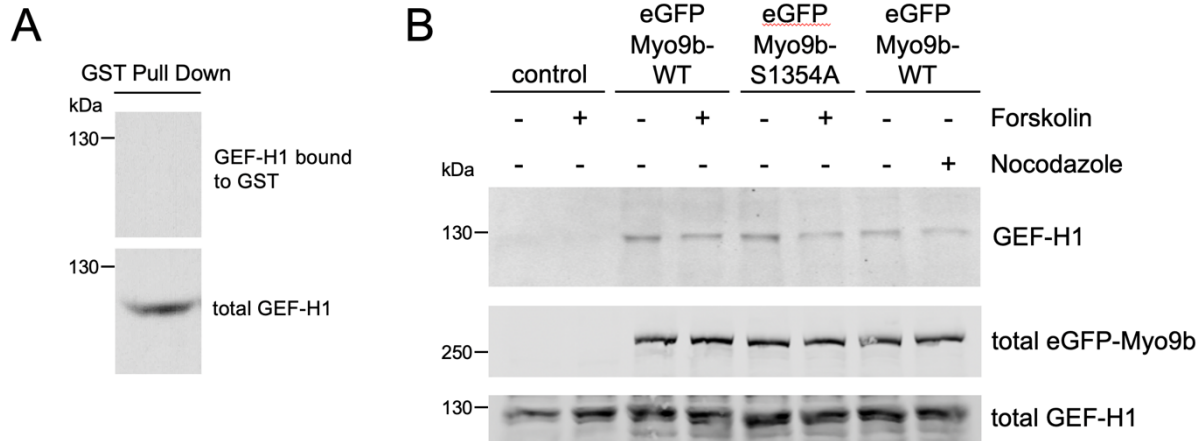
Comer et al. Supplementary Figure 1

Supplementary Figure 1. (Ai) Washed human platelets (approx. 1.5×10^8 platelets/500 μ l aliquot) were pre-incubated without or with PGE₁ (0.5 μ M, 30 secs) or SNP (10 μ M, 10 min) followed by U46619 (1 μ M, 1 min). Platelets were lysed and 20 μ l of each lysate removed for analysis of total RhoA levels followed by GST-RBD pull down assays on the remaining lysate. Samples were then subjected to SDS-PAGE/Western blotting. RhoA antibody was used to detect RhoA-GTP (upper panel) and total RhoA (lower panel) levels using ECL and X-ray film exposure. Data are representative of three independent experiments. **(Aii)** Western blots of experiments shown in (Ai) were analysed by densitometry and the ratios of RhoA-GTP *versus* total RhoA were calculated. Data are expressed as means \pm SD. Statistical significance of the ratio of RhoA-GTP versus total RhoA was determined by ordinary One-Way ANOVA and Bonferroni post-test (U46619 vs U46619/SNP; $**p < 0.001$; U46619 vs U46619/PGE₁; $*p < 0.01$) (U46619 vs control; $\#p < 0.001$). **(B)** Washed human platelets were treated with PGE₁ (0.5 μ M) for 30 seconds and then lysed. Lysates were then subjected to SDS-PAGE with a 13% acrylamide gel followed by Western blotting. Membranes were cut, incubated with anti-RhoA or anti-RhoA pS188 (Biorbyt) antibodies (as highlighted) and realigned for detection. The RhoA band (approx. 21 kDa) and a 15 kDa band detected by the anti-RhoA pS188 (Biorbyt) antibody are denoted by arrows. Data shown are representative of three independent experiments. **(C)** HEK293T cells expressing 3HA-RhoA were incubated without or with forskolin (10 μ M, 10 min) and lysed. Following SDS-PAGE, blots were subjected to immunoblotting with anti-RhoA pS188 (Abcam; upper panel) or anti-RhoA (lower panel) antibodies. Data shown are representative of three independent experiments. **(D)** Washed human platelets were incubated without or with PGE₁ (0.5 μ M, 30 sec), forskolin (10 μ M, 10 min) or SNP (10 μ M, 10 min) and lysed. Aliquots of samples were subjected to Phos-tag PAGE followed by immunoblotting using an anti-RhoA antibody. This experiment was performed three times.



Comer et al. Supplementary Figure 2

Supplementary Figure 2. (A) eGFP empty vector control or eGFP-Myo9b-WT were expressed in HEK293T cells, immunoprecipitated and incubated with purified catalytic subunit of PKA (PKA-Cα) in the presence of [γ - 32 P]ATP for 90 sec. Samples were subjected to SDS PAGE and blotting. Radiolabelled Myo9b was detected by autoradiography (upper panel) and total Myo9b levels were determined using anti-GFP antibody (lower panel). This experiment was performed once and is expanded to highlight the eGFP control for Fig. 2A. (B) Washed human platelets were incubated in the presence of SNP (10 μ M, 10 min) and lysed. Lysates were incubated without or with λ protein phosphatase (λ PP) for 60 min at 30°C. Aliquots of samples were analysed by Phos-tag PAGE followed by immunoblotting using an anti-Myo9b antibody with ECL and film detection. Non-PKG phosphorylated Myo9b (p1), phosphorylated Myo9b (p2) and dephosphorylated Myo9b (b) are denoted by arrows. Data are representative of 3 independent experiments. (C) HEK293T cells expressing eGFP-Myo9b-WT were lysed and lysates were incubated without or with λ protein phosphatase (λ PP) for 60 min at 30°C. Aliquots of samples were subjected to Phos-tag PAGE followed by immunoblotting using anti-GFP antibody. Appearing eGFP-Myo9b-WT bands were labelled as p1 (without λ PP) or b (with λ PP). Data are representative of 4 independent experiments. (D) Alignment of Myo9b sequences from human and rat using Clustal Omega multiple sequence alignment. The highly conserved phosphorylation site (S1354 in human, S1327 in rat) is highlighted by the red box. This conserved region in human contains the RRTpSF sequence that conforms to the PKA/PKG consensus sequence (R-R/K-x-pS/pT). Uniprot accession numbers of sequences; human, Q13459; rat, Q63358.



Comer et al. Supplementary Figure 3

Supplementary Figure 3. (A) Washed human platelets were lysed and subjected to pull-down assays using GST alone. Precipitated, (GST bound, top panel) and total (lower panel) GEF-H1 were detected by Western blotting using an anti-GEF-H1 antibody. (B) eGFP empty vector control, eGFP-Myo9b-WT or eGFP-Myo9b-S1354A were expressed in HEK293T cells then incubated without or with forskolin (10 μ M, 10 min) and lysed. Separately, eGFP-Myo9b-WT expressing cells were treated with nocodazole (10 μ M, 10 min). eGFP-Myo9b-WT and eGFP-S1354A were immunoprecipitated followed by SDS-PAGE and Western blotting. Levels of endogenous GEF-H1 bound to eGFP-Myo9b were determined using an anti-GEFH1 antibody (top panel). Total eGFP-Myo9b (middle panel) and total endogenous GEF-H1 (bottom panel) levels were detected using anti-GFP and anti-GEF-H1 antibodies, respectively. Detection was performed using the LI-COR Odyssey scanning system. Shown are representative data of three independent experiments.